Antagonism of HOX/PBX Dimer Formation Blocks the *In vivo* Proliferation of Melanoma

Richard Morgan,[1] Patricia Macanas Pirard,[1] Liesl Shears,[1] Jastinder Sohal,[2] Ruth Pettengell,[2] and Hardev S. Pandha[1]

[1]Postgraduate Medical School, University of Surrey, Guildford, United Kingdom and [2]St. George's University of London, London, United Kingdom

Abstract

Malignant melanoma is a cancer that arises from melanocyte cells in a complex but well-studied process, and which can only be successfully treated prior to metastasis as it is highly resistant to conventional therapies. A number of recent reports have indicated that members of the HOX family of homeodomain-containing transcription factors are deregulated in melanoma, and may actually be required to maintain proliferation. In this report, we describe the use of a novel, cell-permeable antagonist of the interaction between HOX proteins and PBX, a second homeodomain-containing transcription factor that modifies HOX activity. This antagonist can block the growth of murine B16 cells and trigger apoptosis both *in vitro* and *in vivo* when administered to mice with flank tumors. [Cancer Res 2007;67(12):5806–13]

Introduction

Melanoma is a cancer of the melanocytes, a population of melanin-producing cells that reside in the epidermal basement membrane of the skin (reviewed in ref 1). Its superficial location often makes excision the first choice of treatment for malignant melanoma, and is highly successful if done before malignant cells have breached the epidermal basement membrane. After this event though, malignant cells frequently and quickly metastasize, spreading via the sentient lymph nodes to a variety of targets including the lungs and brain. Despite considerable advances in our understanding of melanoma genetics, thus far, there are no effective treatments for metastatic melanoma, and the prognosis after the disease has progressed to this stage is extremely poor (1).

In addition to genes that regulate the cell cycle and cell signaling pathways, there is a growing interest in the deregulation of transcription factors in melanoma. These include transcription factors that have previously been identified as oncogenes, as well as other transcription factors that are expressed primarily in embryonic tissues but maybe re-expressed in malignant cells. Of particular note are the *HOX* genes, a family of homeodomain-containing transcription factors that determine the identity of cells along different embryonic axes, including the developing nervous system and limb (2). *HOX* gene deregulation has been observed in a number of cancers (reviewed in ref 3), including melanomas (4–7).

Mammals have 39 *HOX* genes, many of which have partly or fully redundant functions (2). For this reason, it has generally proven difficult to fully assess the function of *HOX* genes in some contexts using conventional genetic approaches. To overcome this difficulty, we have designed a small, cell-permeable peptide (HXR9) that antagonizes the interaction between HOX and a second transcription factor (PBX), which binds to HOX proteins in paralogue groups 1 to 8. HOX/PBX dimers have significantly greater binding affinity and specificity for target DNA sequences than the HOX monomer alone (8–10). Here, we show that HXR9 triggers apoptosis in melanoma cells both *in vitro* and *in vivo*.

Materials and Methods

Culturing and maintenance of cell lines. B16F10 was cultured as described previously (11). Briefly, cells were maintained in RPMI medium (Life Technologies) supplemented with 10% fetal calf serum, 2 mmol/L of L-glutamine (Life Technologies), and 1% penicillin/streptomycin (Life Technologies). Cells were maintained at 37°C in a 10% CO_2 incubator. "Primary cells" were derived from a visceral malignant melanoma. This was resected and half of the tissue was used to confirm the disease phenotype through standard histopathologic techniques, whereas the second was treated to separate individual cells. These cells were cultured using the same conditions described above for B16F10 except that DMEM replaced RPMI.

Cord blood–derived CD133+ cells were enriched through positive selection using a MiniMACS separation system (Miltenyi Biotec). Enriched hematopoietic stem cells (HSC; 2×10^3) were suspended in 300 μL of Iscove's modified Dulbecco's medium supplemented with 2% fetal bovine serum (Life Technologies/Invitrogen) and were mixed vigorously with 3 mL of MethoCult GF H4434 containing recombinant cytokines and erythropoietin (StemCell Technologies). Cells were incubated with 60 μmol/L of HXR9 or CXR9 at the start of the experiment and the medium was changed after 24 h (start of day 2).

***In vitro* treatments.** Cells were plated at a density of 2.6×10^4 cells/mL in six-well plates in 1.5 mL of media, and were allowed to adhere overnight. Cells received 60 μmol/L of HXR9, or the control peptide CXR9 for 2 h, and were harvested for subsequent analyses. For annexin V and nuclear staining, B16 cells were plated at a density of 9×10^4 cells/mL in 25 cm^2 culture flasks. After 24 h of recovery, flasks for nuclear staining were treated as mentioned above for 2 h. Then, cells were detached using trypsin/EDTA solution (Sigma) and 200 μL aliquots were used to prepare cytospins at 800 rpm for 5 min using a Cytospin 4 (ThermoShandon). Cells used for annexin V staining were treated with 60 μmol/L of HXR9 alone for 2 h or after the pretreatment with Z-VAD-fmk (50 μmol/L; Bachem) for 45 min. RNA extraction was done using a Qiagen kit.

cDNA synthesis. RNA was reverse-transcribed as described previously. Briefly, RNA was first denatured by heating to 65°C for 5 min. One to five micrograms of RNA was incubated in a volume of 50 μL at 37°C for 1 h with final concentrations of 10 mmol/L of DTT, 1 mmol/L of deoxynucleotide triphosphate mix, as well as 100 μg/μL of poly-T primers, 200 units of reverse transcriptase (Invitrogen), and 40 units of RNaseOUT (Invitrogen). The cDNA synthesis reaction was terminated by placing tubes at 65°C for 5 min.

Real-time PCR. Quantitative reverse transcription-PCR was done using the Stratagene MX4000 real-time PCR machine. The Stratagene MX4000

Note: Supplementary data for this article are available at Cancer Research Online (http://cancerres.aacrjournals.org/).

Requests for reprints: Richard Morgan, Postgraduate Medical School, University of Surrey, Manor Park, Guildford GU2 7WG, United Kingdom. Phone: 44-1483-688618; Fax: 44-1483-688558; E-mail: r.morgan@surrey.ac.uk.

doi:10.1158/0008-5472.CAN-06-4231

measures PCR product accumulation during the exponential phase of the reaction, prior to the amplification becoming vulnerable to limited reagents and cycling variability. Fluorescence increases in accordance with increasing levels of PCR product.

Half-life determination of HXR9. Each peptide was added to freshly prepared human plasma to a final concentration of 1 mmol/L in a total volume of 40 μL. Samples were incubated at 37°C and reactions were stopped by adding 60 μL of water and 0.9 mL of protein gel loading buffer (Bio-Rad) containing 1% 2-mercaptoethanol, and heating to 95°C for 4 min. Two microliters of each sample were run on a 22% acrylamide gel.

Analysis of cell death and apoptosis. The assessment of cell viability was done using the 3-(4,5-dimethylthiazol-2-yl)-2,5-diphenyltetrazolium bromide (Promega), MTS (Promega) assay or the lactose dehydrogenase (LDH) cytotoxicity detection kit (Roche) according to the manufacturer's instructions. Apoptotic morphology was determined using scanning electron microscopy, fluorescence microscopy, and flow cytometry. Changes in nuclear morphology were assessed by fixing B16 cytospins with ice-cold methanol at room temperature for 5 min. The fixed cells were stained with Hoechst 33258 (2 μg/mL; Sigma) and mounted using Vectashield mounting medium (Vector) and analyzed by fluorescence microscopy (Nikon Eclipse TE 2000-S). B16 cells were also processed using the annexin V-FITC apoptosis detection kit as described by the manufacturer (Oncogene Research Products, Calbiochem). Samples were analyzed using a Beckman Coulter Epics XL flow cytometer (argon laser, excitation wavelength 488 nm, and used FL-1 and FL-3 detectors).

Silencing of c-Fos RNA. B16 cells were seeded at 3×10^4 cells/mL in a 96-well plate and allowed to recover for 24 h. Cells were pretreated with a mixture of oligonucleotides complementary to Fos (asFos) or with a random, noncoding oligonucleotides as a control (ascon) for 2 h at a final concentration of 1 μmol/L. B16 cells were then treated with 60 μmol/L of CXR9 or HXR9 for 2 h and the assessment of cell viability was done using the LDH cytotoxicity detection kit. From these cells, the RNA was isolated and samples analyzed by quantitative PCR.

Mice and *in vivo* trial. B16 cells in exponential growth phase were injected s.c. at a dose of 1×10^6 cells into C57black/6 mice. Tumor growth was monitored daily. Once tumors were established, mice received 10 mg/kg of HXR9 or CXR9 i.v. via the tail vein, twice weekly (10 mice per group). Mice were euthanized when tumor volume exceeded 1,200 mm^3 and tumors were excised and fixed for histopathologic analysis. Control groups received CXR9 and PBS accordingly.

Band shift assays. Whole protein extracts were made from excised tumors and used with double-stranded oligonucleotide probes labeled with streptavidin, based on previously described methods (4). The forward sequences of these oligos were: HP (containing a HOX/PBX consensus binding site)—GGACA AACTG AAGGC AGAGC TGATT TATGG CACAC ACACA AGAAT GGACA AACCC GTGAG, HPC (containing an altered HOX/PBX binding site as a control)—GGACA AACTG AAGGC AGAGC GCTCC GTTAA CACAC ACACA AGAAT GGACA AACCC GTGAG. Complexes were supershifted using the anti-PBX1,2,3 antibody (c-20; Santa Cruz Biotechnology) at a dilution of 1:2,000.

Statistical analysis of the data. Data are given as means ± SE of three independent experiments. Comparison of treatments against controls was made using one-way ANOVA followed by Fisher's LSD post hoc test with the SPSS statistical package. The significance level chosen was $P < 0.05$.

Results

HXR9: an antagonist of HOX/PBX interaction. In order to block PBX-dependent HOX function, we designed a cell-permeable peptide that mimics the "hexapeptide" sequence found in HOX proteins of paralogue groups 1 to 9 (8–10, 12–16). The rationale for this design was that HXR9 should act as a specific, competitive inhibitor of the HOX/PBX interaction, and thus prevent HOX/PBX dimers from binding to DNA. For cell penetration, the hexapeptide was linked to a polyarginine (R9) sequence, which has previously been shown to act as an efficient peptide delivery system (17). As a control, we designed a second peptide, CXR9, which lacks a functional hexapeptide portion. In order to increase the stability of these peptides, the NH_2-terminal- and COOH-terminal–most amino acids were synthesized as D-isomers.

The stability of the peptides was assessed by incubating each with human plasma at 37°C. The amounts of peptide remaining after different lengths of time were assessed by SDS-PAGE, and indicated that the half-life of both HXR9 and CXR9 was ~12 h (Supplementary data 1).

In order to test the specificity of HXR9, we treated murine B16 melanoma cells with 60 μmol/L of HXR9 or CXR9 for 1 h and extracted protein from the cells. HOXD9, a known PBX-binding partner that is expressed in melanoma (7), was then immunoprecipitated using an anti-PBX antibody. This technique permits the recovery of HOXD9 in CXR9-treated cells but not in HXR9-treated cells, indicating that HXR9 does indeed block the interaction between PBX and HOX (Fig. 1*A*). As a further control on specificity, we also immunoprecipitated the glucocorticoid receptor (GR). This binds to PBX through an interaction that does not depend on the presence of the hexapeptide motif in the GR protein (18), and thus, this particular interaction should not be blocked by HXR9, and indeed, it is not (Fig. 1*A*).

As an additional test of the peptide's selectivity, we studied its binding to a double-stranded DNA probe containing a HOX/PBX consensus binding site. If the hexapeptide does prevent the interaction of HOX and PBX, it should also disrupt the binding of these proteins to HOX/PBX DNA consensus sites. In order to test this, a band-shift type assay was used. B16 cells were treated with 60 μmol/L of HXR9 or CXR9 for 1 h, and then a cell-free extract was prepared. A streptavidin-labeled DNA probe was added that contains either a HOX/PBX consensus site (HP) or a modified sequence that does not match the consensus site (HPC; Fig. 1*B*). The addition of the HP probe to the CXR9 or control B16 lysates, followed by resolution on a nondenaturing acrylamide gel resulted in a significant reduction in mobility. This indicates that one or more proteins had bound to it. In order to characterize these proteins, a "supershift" assay was done, whereby an anti-PBX antibody was added to the lysate. This resulted in a further shift in mobility equivalent to a single antibody molecule binding, and indicating that each probe-binding protein complex contains a single PBX protein.

Importantly, whereas proteins in the cellular extracts from untreated and CXR9-treated cells bound to the probe, those from the HXR9 extracts did not. This suggests that HXR9 does indeed prevent the formation of HOX/PBX dimers and their subsequent binding to DNA.

In order to confirm that HXR9 can penetrate B16F10 cells, we used an anti-HXR9 antibody combined with the fluorescent FITC tag to examine its intracellular distribution (Fig. 1*D*). This shows that HXR9 is present both in the cytoplasm and the nucleus.

HXR9 triggers apoptosis in B16 and primary melanoma cells. We investigated the antiproliferative activity of HXR9 on B16 cells. The IC_{50} for HXR9 and CXR9 were found to be 20 and 200 μmol/L, respectively. Cells treated with 60 μmol/L of HXR9 for 2 h exhibited a notable change in morphology, including a reduction in dendritic processes (data not shown). Staining with Hoechst dye also revealed a large number of HXR9-treated cells displaying nuclear apoptotic morphology (chromatin condensation; Fig. 2*A*). An additional sign of apoptosis is the appearance of phosphatidylserine in the cytoplasmic surface of the cell membrane (19). This can be detected by fluorescently labeled

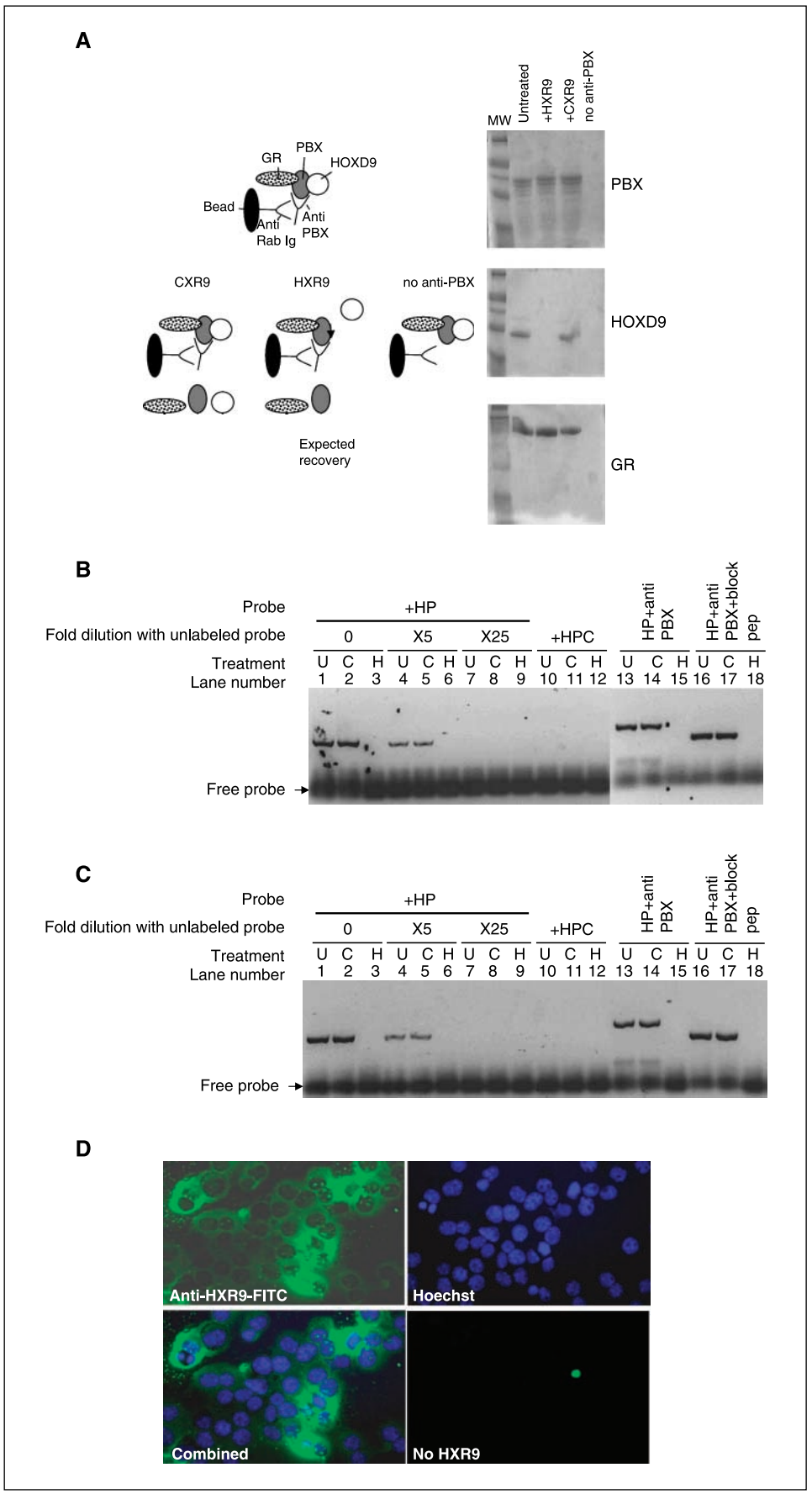

Figure 1. The specificity of hexapeptide action. *A,* HXR9 blocks the binding of HOXD9 to PBX. B16 murine melanoma cells were treated with 60 μmol/L of HXR9 or CXR9 for 4 h. Protein was then extracted from these cells using standard methods, and PBX proteins were precipitated using an anti-PBX antibody. Precipitates were probed for HOXD9, GR, and PBX. HXR9 blocks the binding of PBX to HOXD9 but not to GR. *B,* HXR9 prevents the formation of HOX/PBX/DNA complexes in cultured B16 cells. Double-stranded oligodeoxynucleotide probes were incubated in protein extracted from B16 cells. One of these probes (*HP*) contained a HOX/PBX consensus binding region (in boldface)—5′ CTGTT**TGATT TATTT**GTTTA 3′. A second, control probe (*HPC*) contained an altered HOX/PBX binding site that was not predicted to bind HOX and PBX proteins—5′ CTGTTACTGA CGA**TT**GTTTA 3′. The cells were treated for 2 h with 60 μmol/L of HXR9 (*H*) or with 60 μmol/L of CXR9 (*C*), or were untreated (*U*). Protein extracted from cells treated with the control CXR9 peptide caused a mobility shift in HP (*lane 2*) that could be abolished by 25-fold excess unlabeled HP (*lane 8*), and enhanced (supershifted) by anti-PBX antibody (*lane 14*). This supershift was abolished by the inclusion of a blocking peptide that prevented anti-PBX antibody from binding to PBX (*lanes 16–18*). The mobility of HPC was unchanged by incubating with the protein extract (*lane 11*). Protein extracted from HXR9-treated cells did not change the mobility of HP (*lane 3*) or HPC (*lane 12*), and the mobility of HP was also unchanged in response to unlabeled probe (*lane 9*) or anti-PBX antibody (*lane 15*). *C,* HXR9 prevented the formation of HOX/PBX/DNA complexes in tumors. Tumors injected with HXR9 or CXR9 (10 mg/kg) were used to make cell-free lysates for band shift experiments. The lanes are labeled as above (*B*). *D,* HXR9 enters the cytoplasm and nuclei of B16F10 cells *in vitro*. B16F10 cells were incubated with 60 μmol/L of HXR9 for 2 h and then stained using either an anti-HXR9 antibody labeled with the FITC fluorescent probe (*green, Anti-HXR9-FITC*), with Hoechst (*blue, Hoechst*), or with a combination (*Combined*). As a negative control, B16F10 cells that had not been treated with HXR9 were also stained with anti-HXR9-FITC (*No HXR9*).

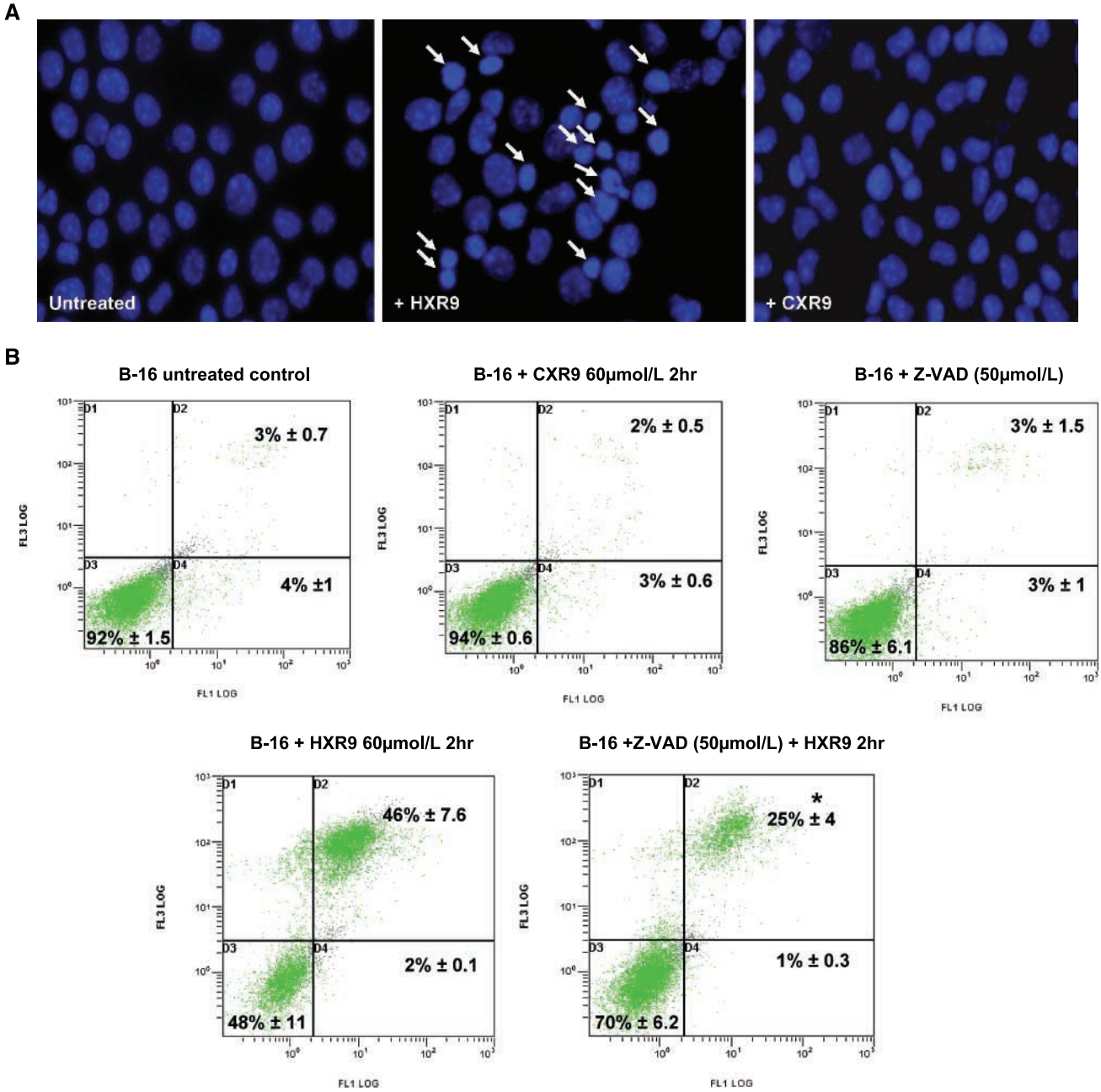

Figure 2. *A,* nuclear staining micrographs of B16 cells treated with HXR9 or CXR9 for 2 h, fixed and stained with Hoechst 33258, and visualized by fluorescence microscopy. *Arrows,* cells that are undergoing apoptosis, the nuclei of which have a continuously bright appearance (as opposed to the speckled pattern in other cells). Magnification, ×400. *B,* flow cytometric analysis of Annexin V-FITC–stained B16 cells treated with 60 μmol/L of HXR9 alone or after pretreatment with Z-VAD-fmk (50 μmol/L) or CXR9 for 2 h, counterstained with PI. Data are the mean ± SE of three independent experiments. *Fl1 axis,* annexin staining (measure of apoptotic changes in the membrane); *FL3 axis,* PI staining (measure of cell permeability). *, $P < 0.05$, significantly different from HXR9 treatment (60 μmol/L for 2 h). *C,* light micrographs of primary melanoma cells treated with 60 μmol/L of CXR9 or HXR9 for 2 h (*top*). Hoechst staining of similarly treated cells revealing the formation of apoptotic bodies (*arrowheads, bottom*). *Bar,* 20 μm.

Annexin V protein and cell sorting using fluorescence-activated cell sorting. Using this technique with B16F10 cells treated for 2 h with 60 μmol/L of HXR9 revealed that a significant proportion of cells were in late phases of apoptosis (Fig. 2*B*). A significant protection from HXR9-induced cell death by apoptosis was observed by the pretreatment of B16F10 cells with the pan-caspase inhibitor Z-VAD-fmk (Fig. 2*B*). CXR9 had no effect on proliferation and did not cause apoptosis.

In addition to the derived B16 murine melanoma cells, we also tested the ability of HXR9 to trigger apoptosis in primary melanoma cells derived from a human malignant melanoma removed for histologic analysis. Cells were separated from this tissue and cultured until they reached 80% confluence and then treated with 60 μmol/L of HXR9 for 2 h, after which they exhibited morphology consistent with cell death (Fig. 2*C*). Staining of nuclei with Hoechst dye also revealed the presence of apoptotic morphology (Fig. 2*C*). Additionally, an IC_{50} determination for HXR9 was done using the LDH cytotoxicity assay. This revealed that the IC_{50} for the cells was 50 μmol/L.

HXR9 causes specific transcriptional changes. In order to examine changes in gene transcription on HXR9 treatment, B16F10 cells were treated for 2 h with 60 μmol/L of HXR9 or CXR9. RNA was extracted for analysis by Microarray, using the Mouse Genome 430A 2.0 Array (Affymetrix), which contains 14,000 characterized mouse genes. Although the majority of genes failed to show any significant changes in transcription, 22 showed an increase in transcription ($P < 0.05$). Most notably, these included oncogenes *Fos* and *Jun*. In order to confirm that these genes were up-regulated in HXR9-treated B16 cells, quantitative PCR was used to measure the relative number of transcripts in RNA extracted from cells (Fig. 3*A*); this confirmed that *Fos, Jun, Dusp1*, and *Atf1* were all significantly up-regulated in response to HXR9.

HXR9 blocks tumor growth and triggers apoptosis *in vivo*. The B16 F10 murine tumor is a well-established experimental *in vivo* model of melanoma, and is also one of the most aggressive murine tumors (20, 21). Subcutaneous inoculation was used to introduce 1×10^5 cells, and mice were treated with twice weekly i.v. doses of HXR9 or CXR9 at 10 mg/kg once tumors were palpable (10 mice per group). At the end point of these experiments, HXR9-treated tumors showed a significant degree of growth retardation (Fig. 4*A*), and histologic analyses of excised tumors revealed a significantly higher level of cell death in HXR9-treated mice (Fig. 4*B*).

In order to assess whether the hexapeptide could block HOX/PBX binding *in vivo*, tumors were injected directly with HXR9 at 10 mg/kg, and were then used to produce nuclear lysates 2 h after treatment. Band shift assays (as detailed above) revealed that protein extracted from these tumors could not bind a DNA probe containing a HOX/PBX consensus binding site, whereas an equivalent extract from CXR9-treated tumors could (Fig. 1*C*), indicating that HXR9 specifically disrupts the formation of HOX/PBX/DNA complexes *in vivo*. Quantitative PCR analysis of RNA extracted from these tumors revealed that *Fos, Jun, Dusp1*, and *Atf3* were up-regulated, mirroring those results obtained *in vitro* (Fig. 3*B*).

Up-regulation of *Fos* is a key event in HXR9-mediated apoptosis. Previous studies have suggested that an increase in *Fos* transcription could trigger apoptosis (22–29). We therefore tested whether *Fos* up-regulation might be responsible for HXR9-mediated apoptosis by ablating *Fos* RNA in B16 cells prior to HXR9 treatment by incubating cells with a mixture of antisense oligonucleotides that were complementary to *Fos* (asFos), and with a second set of random, noncoding oligonucleotides as a control

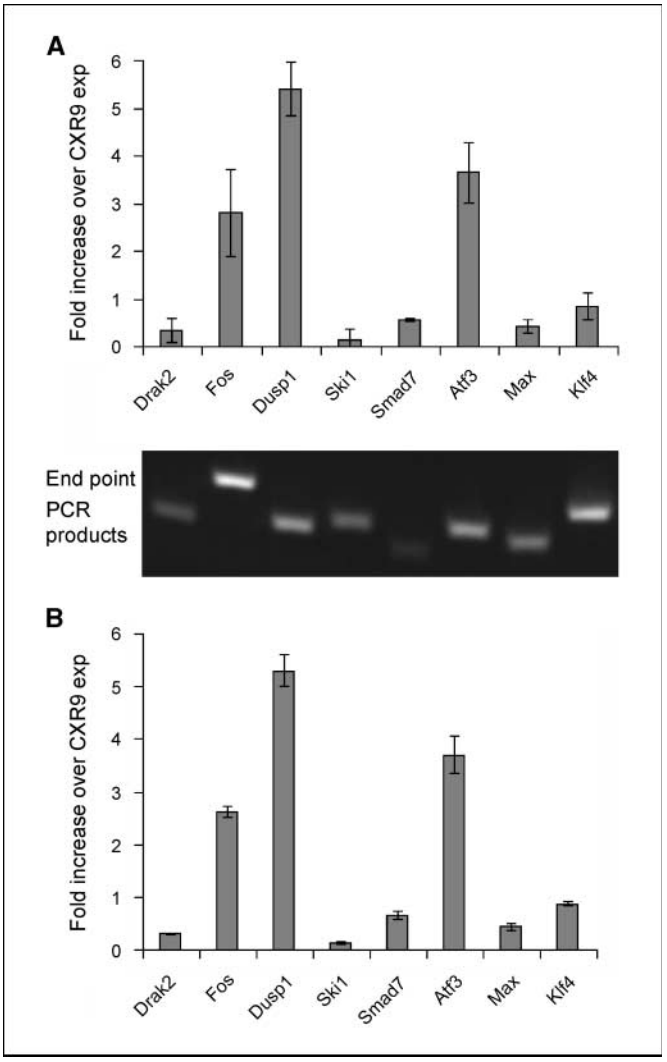

Figure 3. Semiquantitative PCR of those genes identified by microarray as being up-regulated in response to HXR9. RNA extracted from B16 cells cultured *in vitro* and treated with 60 μmol/L of peptide for 2 h (*A*), and B16 tumors injected directly with peptide at 10 mg/kg body weight (*B*); tumors were excised and RNA was extracted 2 h after treatment. Results are expressed as the fold increase in transcript number in HXR9-treated cells above the value for CXR9-treated cells. *A,* the results are an average of two separate experiments; *B,* the results are an average for tumors taken from three individual mice. *Columns,* means; *bars,* SE. "End point" PCR products were resolved on a 2% agarose gel to show that each is a single band (*A, bottom*).

(ascon). Treatment with the former caused a reduction in *Fos* mRNA in HXR9-treated cells to a level that was equivalent to that found in CXR9-treated cells, whereas the ascon set did not (Fig. 5*A*). This reduction in the number of *Fos* transcripts resulted in a partial but significant protection from HXR9-induced cell death (Fig. 5*B*).

HXR9 does not trigger apoptosis in CD133+ cells derived from human umbilical cord blood. A number of previous studies have indicated that *HOX* genes are essential in the correct proliferation and differentiation of blood progenitor cells. In particular, HOXB4 has been shown to promote the proliferation of highly purified populations of HSC (30, 31). In light of these observations, we decided to test the toxicity of HXR9 on a population of cells affinity-purified from human umbilical cord blood using CD133, a marker of primitive blood progenitor cells (32). CD133+ cells continued to proliferate when treated with

HXR9, although at a lower rate than CXR9-treated cells (Fig. 6), and no significant differences in cell death were observed for the two treatments (data not shown).

No overt toxicity was apparent in HXR9-treated mice. HXR9 toxicity was assessed by i.v. administration to MF-1 mice at 15 mg/kg for 10 days. As *HOX* gene function is important in hemopoiesis, close attention was paid to potential adverse affects in the bone marrow and peripheral blood. Peripheral blood samples were taken prior to administering HXR9. After 10 days of treatment consisting of daily i.v. doses of 15 mg/kg, no adverse side effects were seen in HXR9- or CXR9-treated mice. Full blood counts were within expected reference ranges seen in the strain of mice used, and histologic analysis of the liver also revealed no abnormalities (data not shown).

Discussion

In this study, we have shown that antagonizing the interaction between HOX and PBX proteins triggers apoptosis in malignant melanoma cells, both *in vitro* and *in vivo*. *HOX* genes are also known to promote the proliferation of normal HSCs however, raising the possibility that antagonizing the same interaction in these cells could likewise be cytotoxic (30, 31). Our findings indicate that this is not the case though, as purified HSC populations continue to proliferate even in the presence of HXR9, and that there is no overt toxicity observed in mice. These findings concur with previous work indicating that a mutant version of HOXB4 lacking a functional hexapeptide was actually more effective in promoting HSC proliferation than the wild-type sequence (33). Taken together, these results suggest that targeting the interaction between HOX and PBX could be selective for the malignant phenotype, in a way that direct knockout of *HOX* genes would not.

How does antagonizing the HOX/PBX interaction trigger apoptosis in B16 melanoma cells? Microarray analysis of cells treated with HXR9 has identified a number of target genes that become dysregulated, including the oncogene *c-Fos*, the expression of which increases 2.6-fold 2 h after HXR9 treatment. This increase in *c-Fos* transcription must be at least partly responsible for the induction of apoptosis, as knocking down its expression in B16 melanoma cells results in a considerable reduction in their sensitivity to HXR9. *Fos* and its binding partner *Jun* are both members of the bZIP superfamily of transcription factors, which are characterized by a basic DNA-binding domain combined with a leucine zipper region (34). JUN can homodimerize to form the activator protein (AP-1) transcription factor. FOS cannot homodimerize, but it could also form part of the AP-1 transcription factor by binding JUN. AP-1 activates the expression of a number of genes involved in cell cycle regulation, including *cyclin D1* (35). Conversely, AP-1 also mediates apoptosis in a wide range of cell types including lymphocytes, fibroblasts, neurons, and retinal cells (22–29). The mechanistic basis of AP-1–mediated apoptosis is unclear, and depends in part on the actual composition of the AP-1 dimer. Jun-containing AP-1 can promote the transcription of the Fas ligand (FasL), which promotes cell death through the FasL/Fas receptor pathway in lymphocytes, fibroblasts, and neurons (22–26). Fos overexpression induces apoptosis in hepatocytes (36), and is also required for Myc-induced cell death in hepatoma cells (37). Furthermore, the re-expression of Fos in a number of established tumor cell lines can be anti-oncogenic through the activation of proapoptotic genes, although this seems to involve a different mechanism from that used by Jun (38).

In addition to *c-Fos*, a number of other target genes are also up-regulated by HXR9, of which *Dusp1* and *Atf3* show by far the

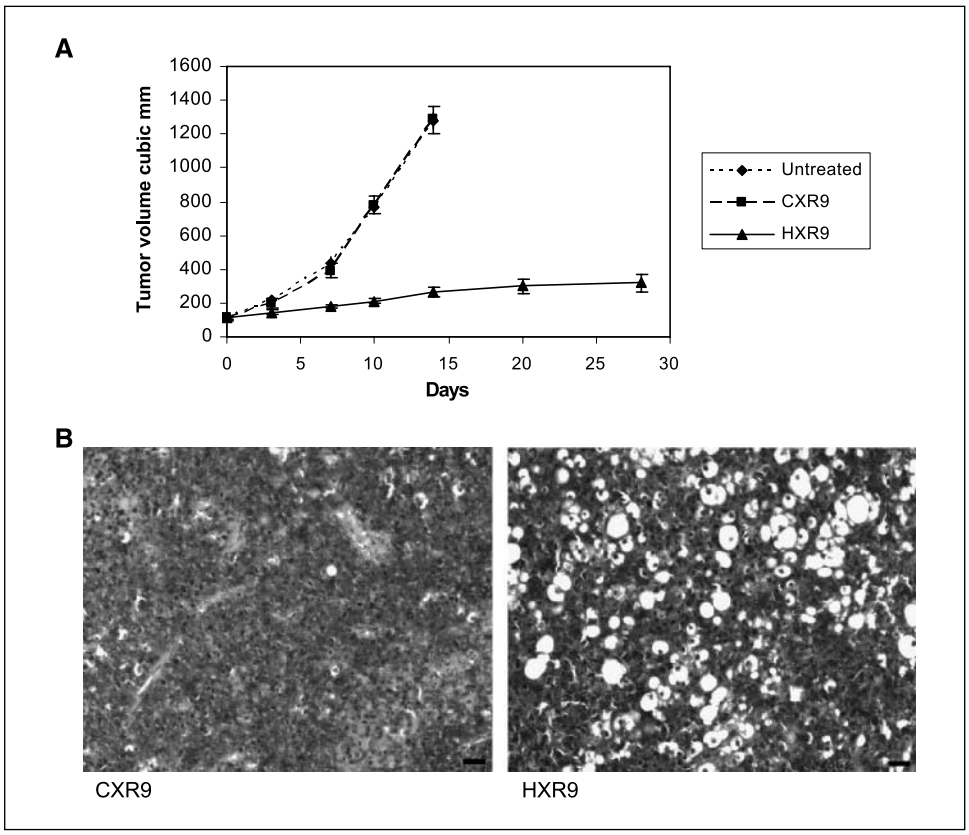

Figure 4. Treatment of melanoma tumors *in vivo*. *A* and *B*, mice were injected with one million B16 cells s.c. and treatment was started when tumors first became palpable (day 0 = first day after treatment). Mice were treated twice weekly with an i.v. dose of 10 mg/kg. *A*, mean changes in tumor size over the treatment period (n = 8); *Points*, means; *bars*, SD. *B*, histologic sections of tumors from HXR9- and CXR9-treated mice at the end of treatment. Sections were stained with H&E. *Bar*, 5 μm.

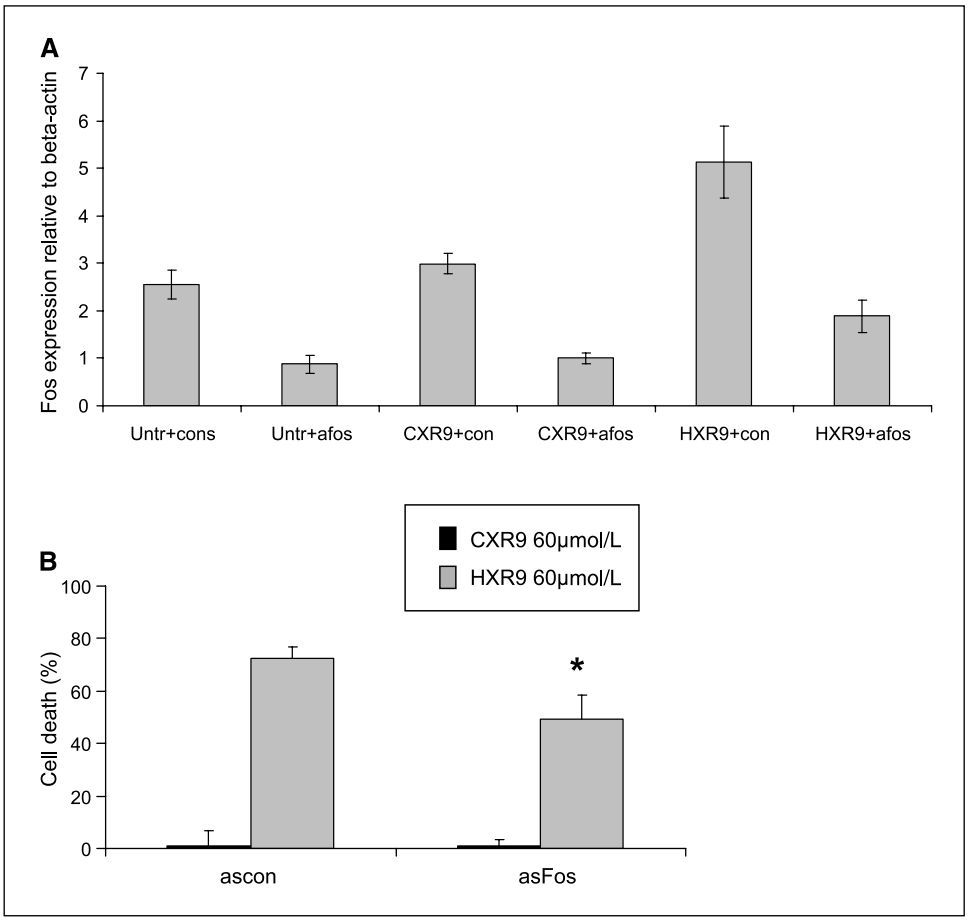

Figure 5. Antisense-mediated reduction in Fos expression protects cells from HXR9. B16 cells were pretreated with control noncoding oligonucleotides (*ascon*) or with a mixture of antisense oligonucleotides complementary to Fos (*asFos*) for 2 h before treatment with 60 μmol/L of CXR9 or HXR9 for 2 h. *A,* RNA was isolated and analyzed by quantitative PCR to assess Fos expression. *B,* LDH cytotoxicity assay to determine the sensitivity of asFos- and ascon-treated cells to HXR9. *Columns,* means of three independent experiments; *bars,* SE; *, $P < 0.05$.

greatest increase. The former encodes a dual specificity phosphatase, a protein that can remove phosphate residues from serine, threonine, and tyrosine residues of a wide range of substrates and can block signaling through the mitogen-activated kinase pathway, thereby blocking cellular proliferation (reviewed in ref. 39). *Atf3* is a member of the activating transcription factor/cyclic AMP–responsive element binding protein family of transcription factors that are known for their role in stress response, including DNA damage (40). It has recently been shown that *Atf3* can stabilize p53 by preventing its ubiquitination (41), and promote its tumor suppressor functions, including the induction of apoptosis (42). *Atf3* also promotes cell cycle arrest and apoptosis in UV-treated fibroblast cells, and blocks Ras-mediated transformation (43).

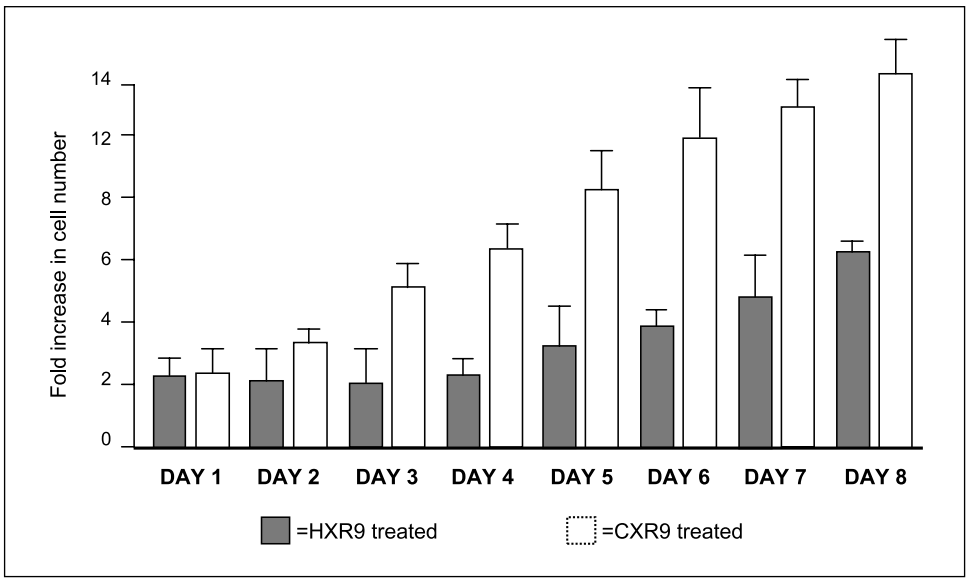

Figure 6. Proliferation of HSCs in response to HXR9. CD133-expressing cells purified from umbilical cord blood were cultured for 8 d with an initial dose of 60 μmol/L of HXR9 or CXR9, and the increase in cell numbers over this time was measured. *Columns,* means of three experiments; *bars,* SE.

Many of the other target genes identified in the screen also have antitumor properties. Kruppel-like factor 4 is a transcription factor that is known to be down-regulated in many colorectal cancers, inhibits the activity of the oncogenic transcription factor β-catenin, and prevents xenograft tumor growth in athymic nude mice (44). *Mad* is an inhibitor of another oncogenic transcription factor, *myc*, and also has a role in blocking proliferation (reviewed in ref. 45). Finally, *Drak2* is a serine/threonine kinase with a high degree of sequence and functional homology to the death-associated kinases involved in apoptosis, and can induce apoptosis when overexpressed in NIH 3T3 cells (46).

The predominance of tumor suppressor and proapoptotic genes among HXR9 targets, together with the ability of HXR9 to induce apoptosis in B16 melanoma cells, suggests that the function of *HOX* gene expression may itself be to inhibit the intrinsic tumor–suppressing pathways. The relative importance of these targets is likely to vary from one cell type to another depending on the genetic background, but a generalized inhibition of many tumor suppressing pathways could account for the wide range of tumors that overexpress *HOX* genes. Together with the data presented here showing that HXR9 could selectively kill malignant cells, these observations suggest that the HOX/PBX interaction may present an important target in cancer therapy.

Acknowledgments

Received 11/17/2006; revised 4/10/2007; accepted 4/19/2007.

Grant support: Association for International Cancer Research (04-382), Cancer Research UK (C7822/A3832), and the Prostate Project.

The costs of publication of this article were defrayed in part by the payment of page charges. This article must therefore be hereby marked *advertisement* in accordance with 18 U.S.C. Section 1734 solely to indicate this fact.

References

1. Chudnovsky Y, Khavari PA, Adams AE. Melanoma genetics and the development of rational therapeutics. J Clin Invest 2005;115:813–24.
2. Krumlauf R. Hox genes in vertebrate development. Cell 1994;78:191–201.
3. Grier DG, Thompson A, Kwasniewska A, et al. The pathophysiology of HOX genes and their role in cancer. J Pathol 2005;205:154–71.
4. Care A, Silvani A, Meccia E, et al. HOXB7 constitutively activates basic fibroblast growth factor in melanomas. Mol Cell Biol 1996;16:4842–51.
5. Cillo C, Cantile M, Mortarini R, Barba P, Parmiani G, Anichini A. Differential patterns of HOX gene expression are associated with specific integrin and ICAM profiles in clonal populations isolated from a single human melanoma metastasis. Int J Cancer 1996;66:692–7.
6. Maeda K, Hamada J, Takahashi Y, et al. Altered expressions of HOX genes in human cutaneous malignant melanoma. Int J Cancer 2005;114:436–41.
7. Svingen T, Tonissen KF. Altered HOX gene expression in human skin and breast cancer cells. Cancer Biol Ther 2003;2:518–23.
8. Chang CP, Shen WF, Rozenfeld S, Lawrence HJ, Largman C, Cleary ML. Pbx proteins display hexapeptide-dependent cooperative DNA binding with a subset of Hox proteins. Genes Dev 1995;9:663–74.
9. Medina-Martinez O, Ramirez-Solis R. *In vivo* mutagenesis of the Hoxb8 hexapeptide domain leads to dominant homeotic transformations that mimic the loss-of-function mutations in genes of the Hoxb cluster. Dev Biol 2003;264:77–90.
10. Shen WF, Rozenfeld S, Lawrence HJ, Largman C. The Abd-B-like Hox homeodomain proteins can be subdivided by the ability to form complexes with Pbx1a on a novel DNA target. J Biol Chem 1997;272:8198–206.
11. Chang MR, Lee WH, Choi JW, Park SO, Paik SG, Kim YS. Antitumor immunity induced by tumor cells engineered to express a membrane-bound form of IL-2. Exp Mol Med 2005;37:240–9.
12. Phelan ML, Sadoul R, Featherstone MS. Functional differences between HOX proteins conferred by two residues in the homeodomain N-terminal arm. Mol Cell Biol 1994;14:5066–75.
13. Piper DE, Batchelor AH, Chang CP, Cleary ML, Wolberger C. Structure of a HoxB1-1 heterodimer bound to DNA: role of the hexapeptide and a fourth homeodomain helix in complex formation. Cell 1999;96:587–97.
14. Shanmugam K, Featherstone MS, Saragovi HU. Residues flanking the HOX YPWM motif contribute to cooperative interactions with PBX. J Biol Chem 1997;272:19081–7.
15. Morgan R. Hox genes: a continuation of embryonic patterning? Trends Genet 2006;22:67–9.
16. Morgan R, In der Rieden P, Hooiveld MH, Durston AJ. Identifying HOX paralog groups by the PBX-binding region. Trends Genet 2000;16:66–7.
17. Jiang T, Olson ES, Nguyen QT, Roy M, Jennings PA, Tsien RY. Tumor imaging by means of proteolytic activation of cell-penetrating peptides. Proc Natl Acad Sci U S A 2004;101:17867–72.
18. Subramaniam N, Campion J, Rafter I, Okret S. Cross-talk between glucocorticoid and retinoic acid signals involving glucocorticoid receptor interaction with the homoeodomain protein Pbx1. Biochem J 2003;370:1087–95.
19. Koopman G, Reutelingsperger CP, Kuijten GA, Keehnen RM, Pals ST, van Oers MH. Annexin V for flow cytometric detection of phosphatidylserine expression on B cells undergoing apoptosis. Blood 1994;84:1415–20.
20. Fidler IJ, Nicolson GL. Tumor cell and host properties affecting the implantation and survival of blood-borne metastatic variants of B16 melanoma. Isr J Med Sci 1978;14:38–50.
21. Shrayer D, Bogaars H, Hearing VJ, Maizel A, Wanebo H. Further characterization of a clinically relevant model of melanoma metastasis and an effective vaccine. Cancer Immunol Immunother 1995;40:277–82.
22. Eichhorst ST, Muller M, Li-Weber M, Schulze-Bergkamen H, Angel P, Krammer PH. A novel AP-1 element in the CD95 ligand promoter is required for induction of apoptosis in hepatocellular carcinoma cells upon treatment with anticancer drugs. Mol Cell Biol 2000;20:7826–37.
23. Kasibhatla S, Brunner T, Genestier L, Echeverri F, Mahboubi A, Green DR. DNA damaging agents induce expression of Fas ligand and subsequent apoptosis in T lymphocytes via the activation of NF-κB and AP-1. Mol Cell 1998;1:543–51.
24. Kolbus A, Herr I, Schreiber M, Debatin KM, Wagner EF, Angel P. c-Jun-dependent CD95-L expression is a rate-limiting step in the induction of apoptosis by alkylating agents. Mol Cell Biol 2000;20:575–82.
25. Le-Niculescu H, Bonfoco E, Kasuya Y, Claret FX, Green DR, Karin M. Withdrawal of survival factors results in activation of the JNK pathway in neuronal cells leading to Fas ligand induction and cell death. Mol Cell Biol 1999;19:751–63.
26. Matsui K, Xiao S, Fine A, Ju ST. Role of activator protein-1 in TCR-mediated regulation of the murine fasl promoter. J Immunol 2000;164:3002–8.
27. Grimm C, Wenzel A, Behrens A, Hafezi F, Wagner EF, Reme CE. AP-1 mediated retinal photoreceptor apoptosis is independent of N-terminal phosphorylation of c-Jun. Cell Death Differ 2001;8:859–67.
28. Hafezi F, Grimm C, Wenzel A, Abegg M, Yaniv M, Reme CE. Retinal photoreceptors are apoptosis-competent in the absence of JunD/AP-1. Cell Death Differ 1999;6:934–6.
29. Rich KA, Zhan Y, Blanks JC. Aberrant expression of c-Fos accompanies photoreceptor cell death in the rd mouse. J Neurobiol 1997;32:593–612.
30. Kyba M, Perlingeiro RC, Daley GQ. HoxB4 confers definitive lymphoid-myeloid engraftment potential on embryonic stem cell and yolk sac hematopoietic progenitors. Cell 2002;109:29–37.
31. Antonchuk J, Sauvageau G, Humphries RK. HOXB4-induced expansion of adult hematopoietic stem cells *ex vivo*. Cell 2002;109:39–45.
32. Kobari L, Giarratana MC, Pflumio F, Izac B, Coulombel L, Douay L. CD133+ cell selection is an alternative to CD34+ cell selection for *ex vivo* expansion of hematopoietic stem cells. J Hematother Stem Cell Res 2001;10:273–81.
33. Beslu N, Krosl J, Laurin M, Mayotte N, Humphries KR, Sauvageau G. Molecular interactions involved in HOXB4-induced activation of HSC self-renewal. Blood 2004;104:2307–14.
34. Hess J, Angel P, Schorpp-Kistner M. AP-1 subunits: quarrel and harmony among siblings. J Cell Sci 2004;11:5965–73.
35. Albanese C, Johnson J, Watanabe G, et al. Transforming p21ras mutants and c-Ets-2 activate the cyclin D1 promoter through distinguishable regions. J Biol Chem 1995;270:23589–97.
36. Mikula M, Gotzmann J, Fischer AN, et al. The proto-oncoprotein c-Fos negatively regulates hepatocellular tumorigenesis. Oncogene 2003;22:6725–38.
37. Kalra N, Kumar V. c-Fos is a mediator of the c-myc-induced apoptotic signaling in serum-deprived hepatoma cells via the p38 mitogen-activated protein kinase pathway. J Biol Chem 2004;279:25313–9.
38. Fleischmann A, Jochum W, Eferl R, Witowsky J, Wagner EF. Rhabdomyosarcoma development in mice lacking Trp53 and Fos: tumor suppression by the Fos protooncogene. Cancer Cell 2003;4:477–82.
39. Ducruet AP, Vogt A, Wipf P, Lazo JS. Dual specificity protein phosphatases: therapeutic targets for cancer and Alzheimer's disease. Annu Rev Pharmacol Toxicol 2005;45:725–50.
40. Wek RC, Jiang HY, Anthony TG. Coping with stress: eIF2 kinases and translational control. Biochem Soc Trans 2006;3:7–11.
41. Yan C, Lu D, Hai T, Boyd DD. Activating transcription factor 3, a stress sensor, activates p53 by blocking its ubiquitination. EMBO J 2005;24:2425–35.
42. Yan C, Boyd DD. ATF3 regulates the stability of p53: a link to cancer. Cell Cycle 2006;5:926–9.
43. Lu D, Wolfgang CD, Hai T. Activating transcription factor 3, a stress-inducible gene, suppresses Ras-stimulated tumorigenesis. J Biol Chem 2006;281:10473–81.
44. Zhang W, Chen X, Kato Y, et al. 2006. Novel cross talk of Kruppel-like factor 4 and β-catenin regulates normal intestinal homeostasis and tumor repression. Mol Cell Biol 2006;26:2055–64.
45. Rottmann S, Luscher B. The mad side of the Max network: antagonizing the function of Myc and more. Curr Top Microbiol Immunol 2006;302:63–122.
46. Sanjo H, Kawai T, Akira S. DRAKs, novel serine/threonine kinases related to death-associated protein kinase that trigger apoptosis. J Biol Chem 1998;273:29066–71.

Antagonism of HOX/PBX Dimer Formation Blocks the *In vivo* Proliferation of Melanoma

Richard Morgan, Patricia Macanas Pirard, Liesl Shears, et al.

Cancer Res 2007;67:5806-5813.